Alloy disorder effects on the electronic properties of III-V quaternary semiconductor alloys

Sylvester N. Ekpenuma, Charles W. Myles, and Jeffrey R. Gregg*
Department of Physics and Engineering Physics, Texas Tech University, P.O. Box 4180, Lubbock, Texas 79409-1051
(Received 17 July 1989; revised manuscript received 21 September 1989)

A coherent-potential-approximation (CPA) formalism for the treatment of III-V quaternary semiconductor alloys with two disordered sublattices is developed. This formalism is applied to the alloys $Al_xGa_{1-x}As_yP_{1-y}$, $Al_xGa_{1-x}As_ySb_{1-y}$, $In_{1-x}Ga_xAs_yP_{1-y}$, and $In_{1-x}Ga_xAs_ySb_{1-y}$, and results are presented for the CPA densities of states, self-energies, band-bowing parameters, and energy-gap variations with composition. Deviations from the virtual-crystal approximation (VCA), which are indications of the effects of alloy disorder, are found to be more significant for the alloys $In_{1-x}Ga_xAs_ySb_{1-y}$ and $In_{1-x}Ga_xAs_yP_{1-y}$ than for $Al_xGa_{1-x}As_yP_{1-y}$ and $Al_xGa_{1-x}As_ySb_{1-y}$. As expected, the amount of disorder as measured by the magnitudes of the self-energy shifts, bowings, and differences between the CPA and VCA energy gaps is stronger at certain alloy compositions than others. Comparison is also made of the experimental energy gap of $In_{1-x}Ga_xAs_yP_{1-y}$ lattice matched to InP, with calculated VCA and CPA energy gaps.

I. INTRODUCTION

Quaternary III-V semiconductor alloys with two disordered sublattices, those whose chemical formulas have the general form $A_xB_{1-x}C_yD_{1-y}$, have important technological device applications. Here x and y are the compositions and A, B, C, and D are the constituent atoms. (In what follows, where possible, we use the notation ABCD to denote the alloy $A_xB_{1-x}C_yD_{1-y}$.) Such materials have, for example, found use in photodetectors for fiber optics communications, in solid-state lasers, in light-emitting diodes, and in high-speed heterojunction transistors.[1-3] A major feature that has made this class of materials valuable for optoelectronic device applications is the fact that the average lattice constant and band gap can be varied independently so that (epitaxial) layers of quaternary alloys of varying compositions can be fabricated on a given lattice-matched substrate.[1,4] By contrast, for ternary alloy systems fabrication of lattice-matched layers is more difficult. This type of fabrication has been successfully accomplished for InGaAsP lattice matched to InP.[1]

To our knowledge, the only detailed theoretical studies of the electronic properties of alloys of this type have been coherent-potential-approximation (CPA) calculations for InGaAsP lattice matched to InP and GaAs. These have been carried out by Chen and Sher for the valence bands only,[5] and more recently for both the valence and conduction bands[6] by Gera *et al.* In addition to these theoretical investigations, various experimental data exist for InGaAsP.[1,2,7] Despite the wealth of information which exists for this material, however, and despite the fact that other quaternary alloys have potential device applications, there have not been any detailed studies of the electronic properties of other III-V quaternary materials of this type. For example, the compositional variation of the band gap and other properties is information which is needed for device design and which is at present not well known for most alloys of this type.

The purpose of this paper is to improve upon this situation by developing a CPA formalism which can be applied to the study of quaternary alloys of the form $A_xB_{1-x}C_yD_{1-y}$, and to apply this formalism to the study of the electronic properties of several III-V alloys of this type. A CPA calculation gives the relative size of the alloy disorder effects in an alloy. A knowledge of such effects can be important for the understanding of transport properties such as electron mobilities and drift velocities in these materials. Hence, such a calculation can be used for a general theoretical characterization of alloys based on the degree of alloy disorder effects.

The CPA formalism we use is a generalization of the Chen and Sher bonding-antibonding CPA formalism.[5,8,9] A bonding CPA approach similar to the present theory was used in Ref. 5 to study the effects of alloy disorder in the valence bands of InGaAsP. The formalism of Ref. 6 utilizes an approach which treats the CPA self-energies for the anion and cation derived s and p states separately, but it is apparently only applicable to cases of lattice-matched compositions. In that reference, the effects of diagonal disorder in the valence and conduction bands in InGaAsP were studied for compositions lattice matched to InP and GaAs. Our formalism, which may be viewed as an extension of the formalism of Ref. 5 to include the effects of alloy disorder in the conduction bands, can be applied generally to quaternary alloys with independent variations of the compositions x and y, and not just to lattice-matched compositions where x and y are some functions of each other. It thus includes the effects of interference between the scattering from the two sublattices of the quaternary alloy.

We present the results of our CPA calculations for InGaAsP for general compositions x and y, as well as for particular compositions which are lattice matched to InP and GaAs. In addition, we present CPA results for InGaAsSb, AlGaAsP, and AlGaAsSb. Our calculations for lattice-matched and non-lattice-matched InGaAsP will serve as a comparison with previous results. Our study of

InGaAsSb is motivated by the small energy gap of its ternary $InAs_{1-x}Sb_x$ constituent which is the smallest of the III-V materials.[10] A room-temperature band gap of 99 meV has been observed[11] for this ternary alloy at $x=0.68$. This small-band-gap feature makes this material a prime candidate for long-wavelength (infrared and near-infrared) photodetector applications.[10,11] For the other materials, our studies will provide results necessary for the understanding of the basic physics of these alloys.

We note that theoretical studies of the electronic properties of several III-V ternary alloys of the form $A_xB_{1-x}C$,[8,9] and of III-V quaternary alloys of the form $A_xB_yC_{1-x-y}D$ (Ref. 12) which utilize the CPA have been carried out. The quaternary semiconductor alloys of the form $A_xB_{1-x}C_yD_{1-y}$ which we study in this paper are quite different from these two alloy types because of the presence of two totally disordered sublattices: a group-III-cation-based sublattice and a group-V-anion-based sublattice. By contrast, the other alloy types each possess an ordered sublattice and a disordered sublattice. The presence of the second disordered sublattice in the alloys of interest here obviously makes the CPA formalism more complex than that for the other alloy types.

For the present study, we assume a completely random quaternary alloy, so that one disordered sublattice contains a random mixture of A and B atoms with probabilities x and $1-x$, respectively, and the other sublattice contains C and D atoms which randomly occupy it with probabilities y and $1-y$, respectively. Our assumption of complete randomness is consistent with the CPA calculational procedure which requires an average over random configurations of constituent atoms. It has been shown in extended x-ray-absorption fine structure (EXAFS) experiments on InGaAsSb (Ref. 13) that short-range-order effects might be important and that not all combinations of the compositions x and y are allowed. Where such deviations from randomness occur, more sophisticated approximations such as the quasichemical equilibrium[14] approximation may become necessary. Such an approximation has been applied to the ternary semiconductor alloys.[15] However, it will not be discussed further here.

II. COHERENT-POTENTIAL-APPROXIMATION FORMALISM

The formalism we present here is a generalization of the Chen-Sher[8] CPA formalism previously applied to ternary alloy semiconductors. To obtain our numerical results, the sp^3s^* semiempirical tight-binding band structures of Vogl *et al.*[16] are used as input into this generalized formalism. A general description of the CPA procedure, originally developed by Soven and Taylor, can be found in various review articles,[17] and so only a brief outline of our theory will be given here.

We note that the bonding-antibonding CPA studies carried out in Ref. 9 utilized the same band-structure parameters that we employ here.[16] In that reference, results were presented for five different ternary alloys at various compositions and were shown to compare favorably to the results of bonding-antibonding CPA studies which used other band structures,[8] to the results of molecular CPA studies which included the effects of off-diagonal disorder,[18] and to experiments. Thus this type of CPA theory combined with the band structures of Vogl *et al.*[16] has been tested for the ternary alloys which are the limiting cases of the quaternaries we consider here. We thus have confidence in the trends that we predict for various quaternary alloys as functions of the alloy compositions.

The starting point of our formalism is the virtual-crystal approximation (VCA) Hamiltonian which has the form

$$H_0=xyH_{AC}+y(1-x)H_{BC}+x(1-y)H_{AD}+(1-x)(1-y)H_{BD}\ , \tag{1}$$

where H_{AC}, H_{BC}, H_{AD}, and H_{BD} are the Hamiltonians for the compound semiconductors AC, BC, AD, and BD, respectively, in a tight-binding representation. The true alloy Hamiltonian H_a is the sum of this VCA Hamiltonian and a random potential V:

$$H_a=H_0+V=H_0+\sum_i v_i\ , \tag{2}$$

where the v_i's are the atomic potentials at each cell site and V is the total random potential. For the following discussion, we cast this potential into a bonding and an antibonding basis,[8,19] so that the atomic pairs that make up a bond in a cell can be described in terms of bonding and antibonding states. In this basis, only diagonal disorder can be conveniently treated. We thus neglect off-diagonal disorder in this paper. Off-diagonal disorder has been treated in the work of Hass *et al.*[18] for ternary alloy semiconductors using a molecular CPA, which includes the effects of disorder on states of different chemical origins. A generalization of the formalism of Ref. 18 to treat off-diagonal disorder in the alloys of interest here would be difficult for arbitrary x and y since that formalism requires the existence of well-defined molecular units. These are missing in the quaternary alloy $A_xB_{1-x}C_yD_{1-y}$ since both sublattices are disordered.

In the CPA one seeks to replace the disordered alloy with a translationally invariant, periodic effective medium. This CPA medium is characterized by a complex, energy-dependent self-energy with real and imaginary parts representing the shifts from the VCA eigenstates and the broadening of the states, respectively. In the CPA, the alloy Hamiltonian H_a is thus replaced by an effective medium Hamiltonian defined by

$$H_{\text{eff}}=H_0+\Sigma(E)\ , \tag{3}$$

where $\Sigma(E)$ is the effective coherent potential (or self-energy) which, like the random potential V, can be cast into a bonding-antibonding basis. In this basis, we denote the bonding and antibonding parts of $\Sigma(E)$ as $\sigma_b(E)$ and $\sigma_a(E)$, respectively. The effective Hamiltonian H_{eff} has the full crystal translational symmetry, and the observable properties of the effective medium and thus of the alloy can be obtained from the configurationally averaged Green's function which is replaced in the CPA with an

effective medium Green's function defined by

$$G_{\text{eff}}(E,\sigma)=(E-H_{\text{eff}})^{-1} . \quad (4)$$

In implementing the CPA, one determines the self-energies σ_b and σ_a from the CPA self-consistency condition.[8,12,17] To do this, one forms the single-cell atomic scattering operator or t matrix

$$t_i^j=u_i^j(1-g_j u_i^j)^{-1} . \quad (5)$$

Here g_j is the site-diagonal matrix element of the configurationally averaged Green's function G_{eff} [Eq. (4)], which can be written as

$$g_j(E,\sigma)=\tfrac{1}{4}\int \frac{D_{\text{VCA}}^j(E')}{E-E'-\sigma_j(E)}dE , \quad (6)$$

where $D_{\text{VCA}}^j(E')$ is the VCA density of states for the valence ($j=b$) or the conduction ($j=a$) band. Also, in Eq. (5), we have defined $u_i^j=(\varepsilon_i^j-\bar{\varepsilon}^j-\sigma_j)$ where $\bar{\varepsilon}$ is defined for either value of j as

$$\bar{\varepsilon}=xy\varepsilon_{AC}+y(1-x)\varepsilon_{BC}+x(1-y)\varepsilon_{AD} +(1-x)(1-y)\varepsilon_{BD} , \quad (7)$$

and the index j has been suppressed for clarity. In Eqs. (5) and (6), i is a cell index which can take on any one of the four values AC, BC, AD, or BD depending on which atomic pair occupies the cell and j is an index denoting bonding and antibonding states, which we will also refer to as the valence-and the conduction-band states, respectively. Thus u_i^j in Eq. (5) can take on the values u_{AC}^j, u_{BC}^j, u_{AD}^j, or u_{BD}^j, with appropriate probabilities. The quantities ε_i^j in Eq. (7) represent the bonding or the antibonding energies of the constituent semiconductors AC, BC, AD, or BD, respectively, and are defined by the relation

$$\varepsilon_i^j=\tfrac{1}{4}\int E D_i^j(E)dE , \quad (8)$$

where $D_i^j(E)$ is the density of states for the bonding or antibonding states for the compound i.

The CPA self-consistency condition requires that on the average, there should be no scattering in the effective medium so that the average t matrix vanishes or

$$\langle t_i^j\rangle=0 , \quad (9)$$

where $\langle t_i^j\rangle$ denotes an average over configurations. When this relation is combined with Eq. (5), one obtains

$$0=xyu_{AB}(1-u_{AB}g)^{-1}+y(1-x)u_{BC}(1-u_{BC}g)^{-1} +x(1-y)u_{AD}(1-u_{AD}g)^{-1} +(1-x)(1-y)u_{BD}(1-u_{BD}g)^{-1} . \quad (10)$$

Since in the bonding-antibonding basis the self-consistency requirement holds separately for the valence- and the conduction-band states, Eq. (10) has the same form in both cases. Thus the index j has been suppressed for clarity. Equation (10) can be further expanded to solve explicitly for σ, resulting in a lengthy nonlinear, integral equation, which must be solved iteratively using standard numerical techniques. This equation is shown in Appendix I. Usually, six to ten iterations are enough for convergence. Before solving Eqs. (6)–(10), all energies are shifted to the vacuum level using experimental photothresholds.[20] These energies before the shift are usually referred to zero at the valence-band maximum so that the shift to the vacuum level accounts for band discontinuities. In presenting and interpreting the results of the calculations, we shift all energies back to the top of the VCA valence-band edge.

For the following discussion, it will be convenient to introduce disorder parameters for the bonding or antibonding states. These are defined as differences in the average bonding and antibonding energies given by Eq. (8). For the alloy $ABCD$, if one (arbitrarily) chooses the the material BD as the reference crystal, three disorder parameters can be defined. They are

$$\delta_{AD}=\varepsilon_{BD}-\varepsilon_{AD} , \quad \delta_{BC}=\varepsilon_{BD}-\varepsilon_{BC} , \quad \delta_{AC}=\varepsilon_{BD}-\varepsilon_{AC} , \quad (11)$$

where the index j has again been suppressed. These disorder parameters are a crude measure of the expected amount of alloy disorder in $ABCD$. A more detailed measure is, of course, the energy-dependent CPA self-energy. However, a knowledge of the disorder parameters of a given alloy enables one to estimate the size of the expected disorder effects before a CPA calculation is performed.

It is well known[18] that the type of bonding-antibonding CPA formalism outlined above averages over the disorder effects within the valence and conduction bands and thus does not properly account for the different chemical origins of states in different energy regions. For example, it is known that s-like states are more strongly affected by disorder than p-like states. This effect is accounted for only in an average way in the bonding-antibonding CPA. This formalism also neglects interband effects which might be important in alloys with narrow band gaps, and, as mentioned above, it also neglects off-diagonal disorder. Because of these limitations, the predictions obtained from the formalism should be taken as a first approximation to the expected effects of alloy disorder on the electronic properties. However, since, with the exception of InGaAsP, there have been no previous studies of such effects in the type of quaternary semiconductor alloys considered here, the present study may be viewed as a first step at beginning to understand such properties. Furthermore, based on results obtained previously using this type of formalism to describe ternary semiconductor alloys[8,9] as well as the valence bands of InGaAsP (Ref. 5) and based on comparison of the results presented below with those obtained by others for InGaAsP,[6] we feel that the trends predicted for the variation of various properties as a function of the alloy compositions and from alloy to alloy should be reliable.

III. RESULTS AND DISCUSSION

We first present results for the alloys AlGaAsSb, AlGaAsP, InGaAsP, and InGaAsSb for the compositions $x = y = 0.50$, which is the regime where all of the constituent compounds of the alloys are equally weighted. In Figs. 1(a)–(d) we show the VCA (dotted curves) and the CPA (solid curves) densities of states for AlGaAsSb, AlGaAsP, InGaAsP, and InGaAsSb, respectively. A general feature observed in these figures is the smoothing of the VCA Van Hove singularities by the CPA. This smoothing is especially significant at the top of the valence bands for the InGaAsSb and AlGaAsSb alloys. This is an indication of appreciable disorder effects in the valence bands of these two alloys, and is typical of the effects of alloy disorder on such peaks.[17]

Such disorder effects can also be related to the magnitudes of the disorder parameters, defined in Eq. (11), for the bonding (valence band) and antibonding (conduction band) states. In Table I, we list the bonding and antibonding energies for the constituent compounds and the magnitudes of the resulting disorder parameters for the valence and conduction bands for various combinations of these compounds that are relevant for the alloys considered here. The table shows, for example, that the valence-band disorder parameters for alloys containing mixtures of AlSb and GaAs, AlAs and AlSb, GaAs and GaSb, and AlAs and GaSb are 1.78, 1.48, 1.06, and 0.76 eV, respectively. The corresponding parameters for the same set of compounds for the conduction band are 0.58,

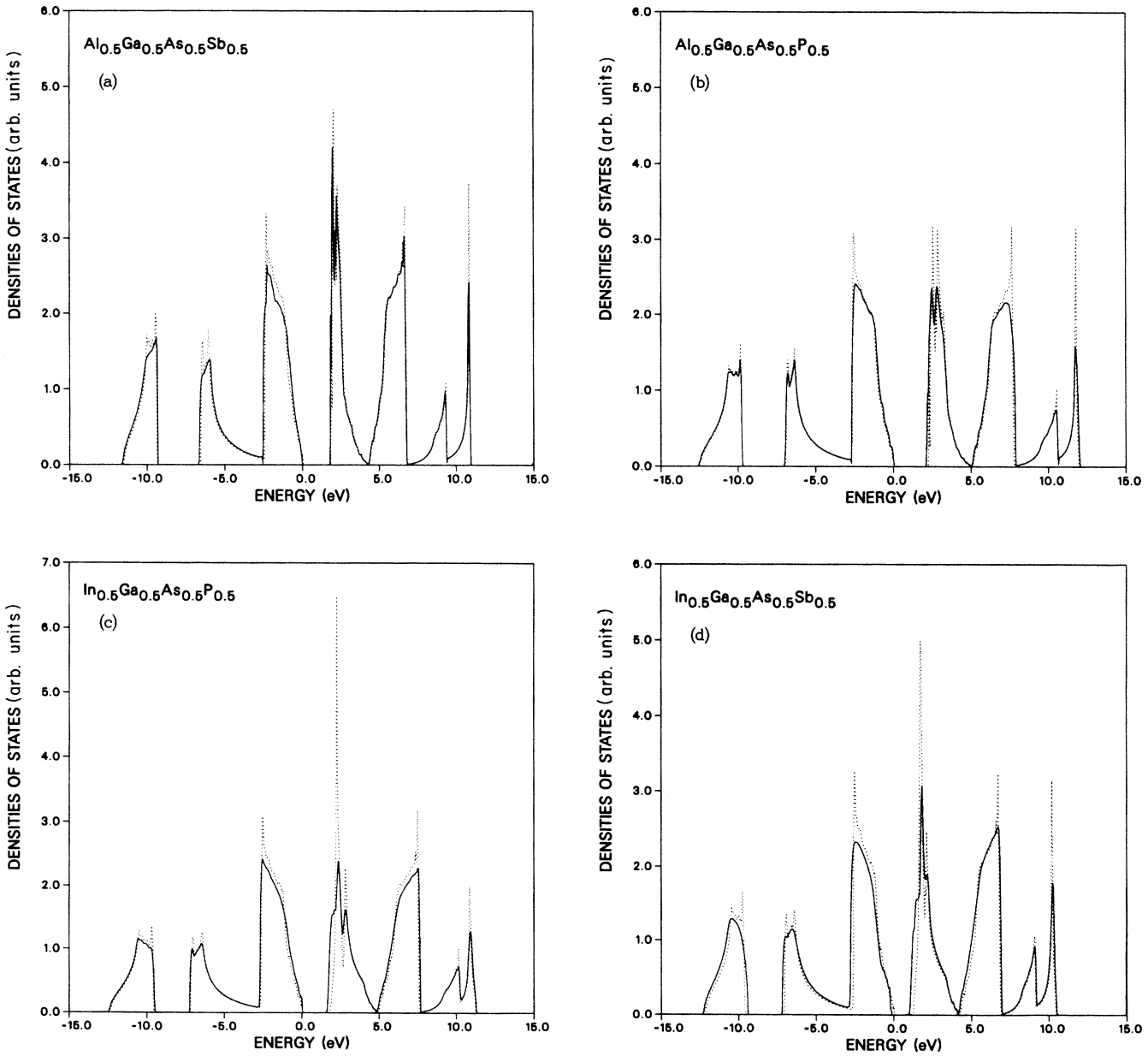

FIG. 1. The CPA (solid curve) and the VCA (dotted curve) density of states for (a) $Al_{0.5}Ga_{0.5}As_{0.5}Sb_{0.5}$, (b) $Al_{0.5}Ga_{0.5}As_{0.5}P_{0.5}$, (c) $In_{0.5}Ga_{0.5}As_{0.5}P_{0.5}$, and (d) $In_{0.5}Ga_{0.5}As_{0.5}Sb_{0.5}$.

0.17, 0.42, and 0.01 eV, respectively. Clearly, these disorder parameter values are in qualitative agreement with the relative amount of the smoothing of the VCA Van Hove singularities by the CPA densities of states curves shown in Figs. 1(a)–1(d).

The self-energies for the same alloys at the same compositions as in Fig. 1 are shown in Figs. 2(a)–2(d), where the solid curves indicate the real parts of the self-energies and the dotted curves are the negative of the imaginary parts. These self-energies are also a measure of the disorder effects in the alloys. Their size is greatest in the InGaAsSb with the magnitude of the real part reaching values of 0.80 eV near the top of the valence band and 0.45 eV near the bottom of the conduction band. The size of the real part of the self-energy of AlGaAsSb rises to about 0.60 eV near the top of the valence band and is almost negligible in the conduction band showing that while the disorder effects for the valence band are appreciable, these effects in the conduction band of this quaternary alloy are minimal. The magnitudes of the self-energies also correlate with the size of the disorder parameters for AlGaAsSb, obtained from Table I. In particular, minimal disorder effects are to be expected from the relatively small disorder parameters. In AlGaAsP, the magnitude of the self-energies rises to a maximum of approximately 0.10 eV about 7.70 eV into the conduction band and fluctuates between zero and 0.05 eV in the rest of the band spectrum. There is therefore small disorder in AlGaAsP, as expected by the small disorder parameters for this alloy. For InGaAsP, a maximum value of 0.20 eV of the self-energy occurs at the top of the valence band; so the disorder in this alloy is stronger than in AlGaAsP. In order to represent these self-energy values for these alloys in plots without obscuring the essential features, the scales have been enlarged [Figs. 2(b) and 2(c)].

The origin and relative sizes of the disorder effects in these alloys as measured by both the self-energies and the disorder parameters can also be related to the differences in the s and p atomic energies which have been used to compute the tight-binding band parameters which we employ in these calculations.[16] For example, the differences in the s atomic energies between In and Ga, between As and P, between Sb and As, and between Sb and P are, respectively, 1.41, 0.28, 2.83, and 3.11 eV, while the differences in the p atomic energies are 0.30, 0.60, 0.95, and 1.55 eV, respectively. As can be seen from Table I, the disorder parameters in alloys containing As and Sb anions are comparatively large (for instance, the valence-band disorder parameter of AlSb and GaAs in AlGaAsSb is 1.78 eV), while disorder is expected to be small for alloys containing As and P. It must be noted that this relation between the relative degree of disorder and the atomic energy differences should not be peculiar

TABLE I. Calculated bonding (valence-band) energies ε_b, antibonding (conduction-band) energies ε_a, and absolute values of disorder parameters $\delta_{b\,(a)}=|\varepsilon^A_{b\,(a)}-\varepsilon^B_{b\,(a)}|$ for III-V semiconductor compounds. All energies are in electron volts.

Compound	ε_b	ε_a	A	B	δ_b	δ_a
AlAs	−10.40	0.04	AlAs	AlSb	1.48	0.17
			AlAs	GaSb	0.76	0.01
			AlAs	GaAs	0.30	0.41
AlSb	−8.92	−0.13	GaAs	AlSb	1.78	0.58
			GaAs	GaSb	1.06	0.42
GaSb	−9.64	0.03	GaSb	AlSb	0.72	0.10
			AlAs	AlP	0.25	0.54
GaAs	−10.70	0.45	AlAs	GaP	0.45	0.70
			GaAs	GaP	0.05	0.28
AlP	−10.65	0.58	GaAs	AlP	0.05	0.13
			GaP	AlP	0.20	0.15
GaP	−10.85	0.73	GaAs	InAs	0.42	0.34
			GaAs	InSb	1.26	0.78
InAs	−10.28	0.11	InAs	GaSb	0.64	0.08
			InAs	InSb	0.84	0.44
InSb	−9.44	−0.33	InSb	GaSb	0.20	0.36
			GaAs	InP	0.55	0.51
InP	−10.15	−0.08	InAs	InP	0.13	0.19
			InAs	GaP	0.57	0.62
			InP	GaP	0.70	0.81

to the band-structure model we use for these calculations but should be the case for other band-structure models where atomiclike (tight-binding) orbitals are used for computing band structures.[19]

Damping of the states (alloy broadening) near the fundamental band gap as represented by the imaginary part (dotted curves) of the self-energy is very small for all of the alloys we have considered. This is in agreement with experimental results.[21] Such alloy broadening is least in AlGaAsP with a maximum value of 0.10 eV occurring about 7.65 eV above the conduction-band minimum (about the same energy where the maximum of the real part occurs), and a maximum in the valence band of 0.06 eV about 2.52 eV below the valence-band maximum. Consistent with results for the real part, values for the imaginary part of the self-energy for the alloy AlGaAsSb are greater in the valence band than in the conduction band, with average values of about 0.25 eV, rising to a maximum of 0.47 eV about 1.75 eV below the valence-band maximum compared to a maximum value of only 0.02 eV about 6.70 eV into the conduction band. In InGaAsP, the maximum value of the imaginary part of the self-energy is about 0.24 eV in both the conduction band (2.20 eV into the conduction band) and the valence band (2.20 eV below the valence-band maximum). In InGaAsSb, maximum values of the imaginary part in the conduction and valence bands are 0.35 and 0.30 eV, respectively, and occur about 1.65 eV into the conduction band and 0.83 eV below the valence-band maximum. These results imply that alloy broadening effects are greater in InGaAsSb than in the other alloys considered here.

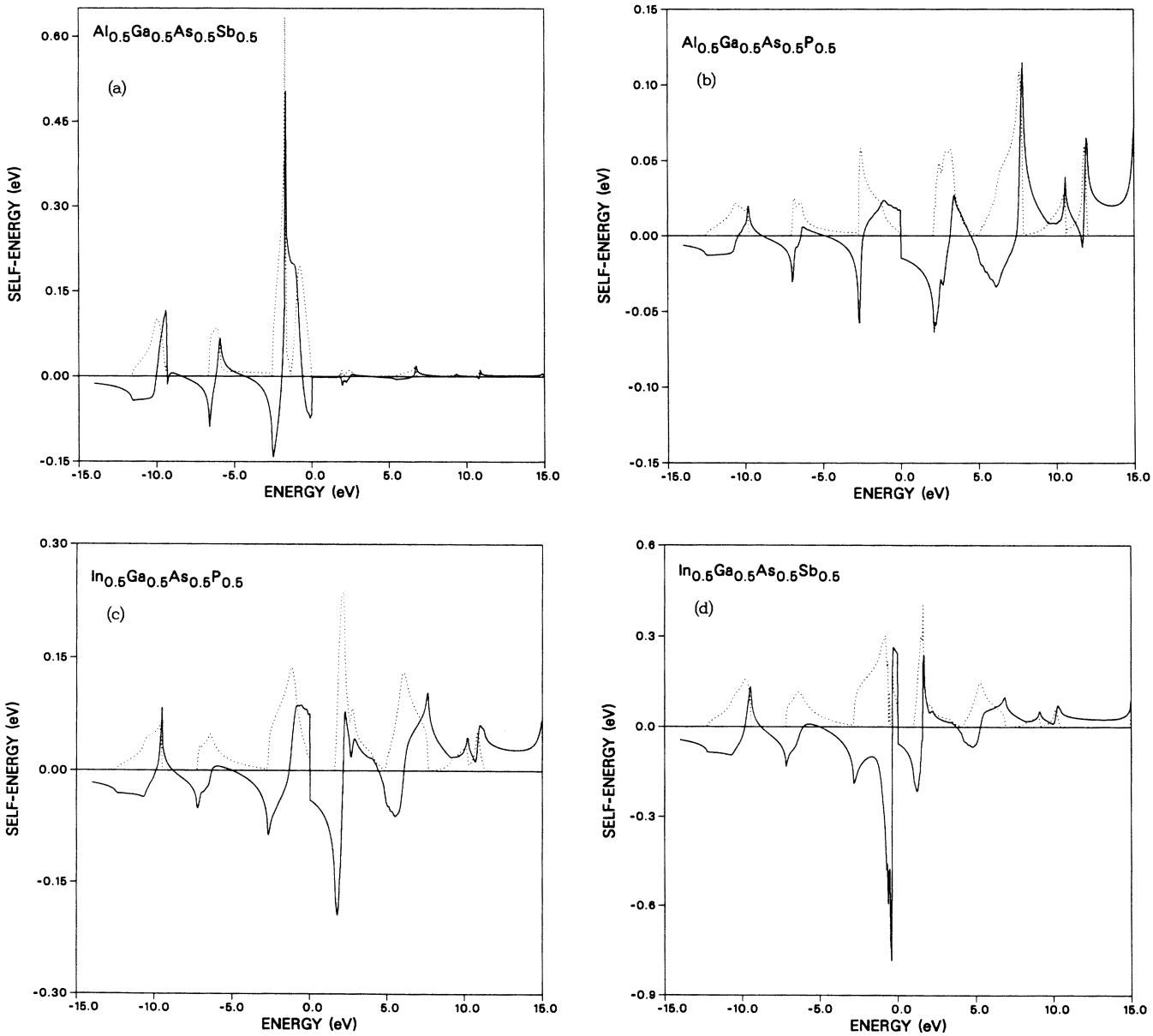

FIG. 2. The real (solid curve) and the negative of the imaginary (dotted curve) parts of the self-energy for (a) $Al_{0.5}Ga_{0.5}As_{0.5}Sb_{0.5}$, (b) $Al_{0.5}Ga_{0.5}As_{0.5}P_{0.5}$, (c) $In_{0.5}Ga_{0.5}As_{0.5}P_{0.5}$, and (d) $In_{0.5}Ga_{0.5}As_{0.5}Sb_{0.5}$.

The band-gap variations with composition in the VCA and CPA are shown for InGaAsP lattice matched to InP ($0 \le x \le 0.47$, $0 \le y \le 1.0$) and to GaAs ($0.48 \le x \le 1.0$, $0 \le y \le 1.0$) in Figs. 3 and 4, respectively. The relations between x and y are $y/x = 2.13$ and $0.42x - 0.22y = 0.2$, respectively, for cases of the InP and GaAs lattice-matched alloys. These figures show that there are deviations of the CPA energy gaps from those predicted by the VCA. The CPA energy gap in the GaAs lattice-matched alloy shows a maximum deviation of 0.18 eV from the VCA energy gap at an As composition y of about 0.40 and a Ga composition $x = 0.69$, while the InP lattice-matched material shows a maximum deviation of 0.09 eV at an As composition between 0.50 and 0.60 and a corresponding Ga composition of approximately 0.26. Also, we have compared our calculated energy gaps for InGaAsP lattice matched to InP (at 0 K) with experimentally measured values[22] at room temperature (Fig. 3). It is seen that the CPA energy gap is a better approximation than the VCA to the experimental data showing that alloy disorder strongly influences the band-gap variation. In particular, if the CPA energy gap is extrapolated to room temperature, it will be in closer agreement with the experiment than Fig. 3 shows.

It is well known that the band edges and band gaps in an alloy deviate from the compositionally weighted averages of those of the constituent compounds. This deviation is called bowing. It is a measure of the variation in the crystal potential across the alloy field,[23] and it exists in both the VCA and the CPA. The deviation between the VCA and the CPA bowing is another measure of alloy disorder. To discuss bowing for the band gap, it is convenient to use the definition of the bowing parameter:[23]

$$E(x,y) = \bar{E} - bf(x,y) , \tag{12}$$

where $\bar{E}$ is the composition weighted average gap, b is called the bowing parameter,[24] and $f(x,y)$ is some quadratic function of the compositions. One method[25] that has been used to calculate bowing in the type of quaternary alloys we consider here treats the disorder on the two sublattices as independent. In this treatment, Eq. (12) is usually written in the form

$$E(x,y) = \bar{E} - b_1 x(1-x) - b_2 y(1-y) , \tag{13}$$

where b_1 and b_2 are two separate bowing parameters. Equation (13) implies that there are two independent contributions to the bowing, one due to the anion sublattice and the second due to the cation sublattice. This is equivalent to the assumption that the two sublattices scatter independently, so that their contributions to the bowing are additive. In this kind of treatment, the effects of interference between the scattering from the two sublattices that serve to reduce the bowing[25] are thus neglected. Such effects should be present even for a perfectly random alloy, as our calculations show. In order to include these effects, we use the more general form given by Eq. (12), and have thus assumed only one bowing parameter. Further, we have used a form of $f(x,y)$ that accounts for the interference effects just mentioned. This form is

$$f(x,y) = x(1-x) + y(1-y) + 1 , \tag{14}$$

which now has an additional term of one that was not in Eq. (13). Using this form of analysis, we have calculated the composition dependence of the band-gap bowing parameters for InGaAsP lattice matched to both InP and GaAs. The results of these calculations are shown in Figs. 5 and 6 for both the CPA (solid curves) and the VCA (dashed curves). The CPA bowing for the InP lattice-matched InGaAsP compares very well with an earlier calculation.[25] However, the magnitude of the

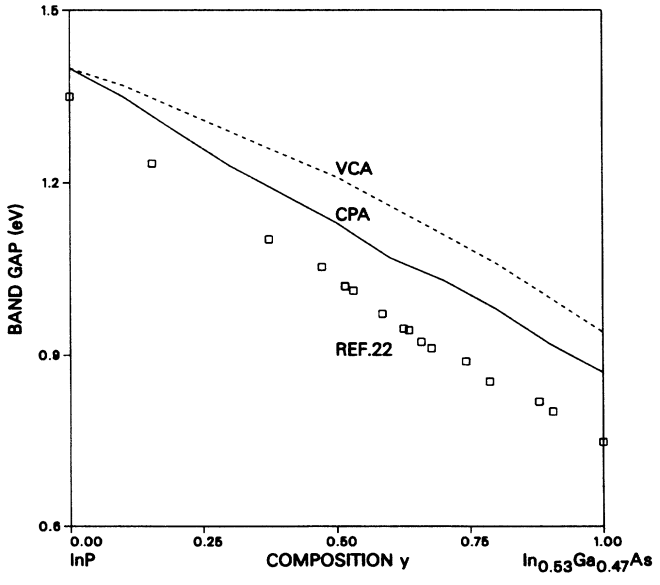

FIG. 3. CPA (solid curve) and VCA (dashed curve) energy-gap variation with As composition y for $In_{1-x}Ga_xAs_yP_{1-y}$ lattice matched to InP ($y/x = 2.13$). These are compared with room-temperature photoluminescence data of Ref. 22.

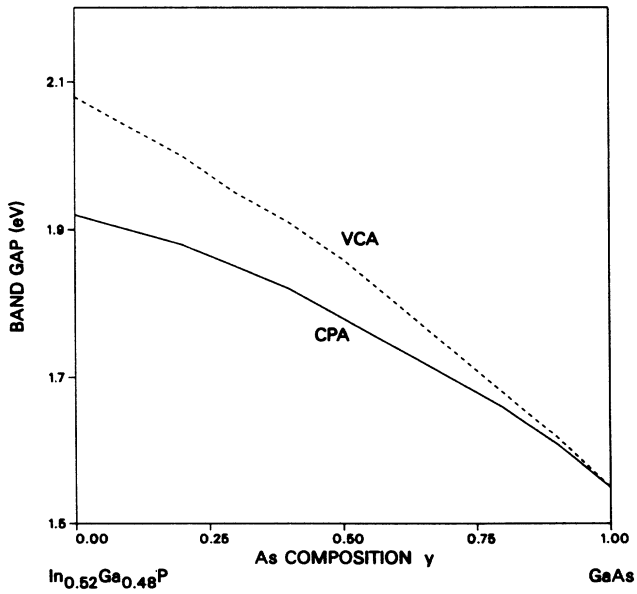

FIG. 4. CPA (solid curve) and VCA (dashed curve) energy-gap variation with As composition y for $In_{1-x}Ga_xAs_yP_{1-y}$ lattice matched to GaAs ($0.42x - 0.22y = 0.20$).

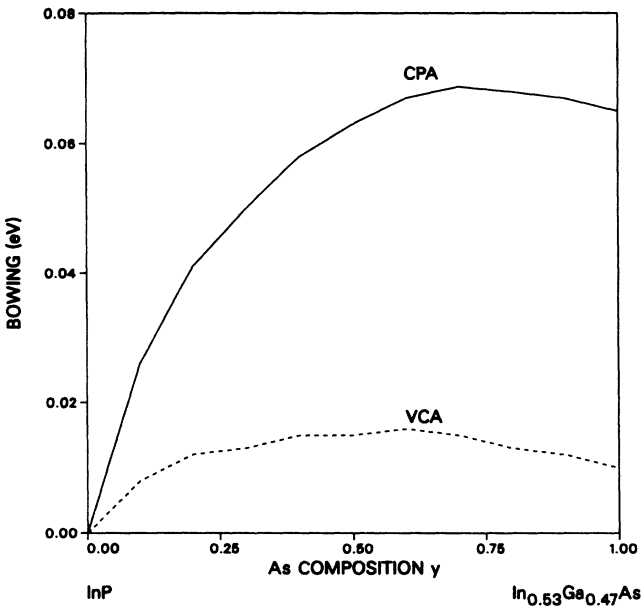

FIG. 5. CPA (solid curve) and VCA (dashed curve) band-gap bowing as a function of As composition y for $In_{1-x}Ga_xAs_yP_{1-y}$ lattice matched to InP ($y/x=2.13$).

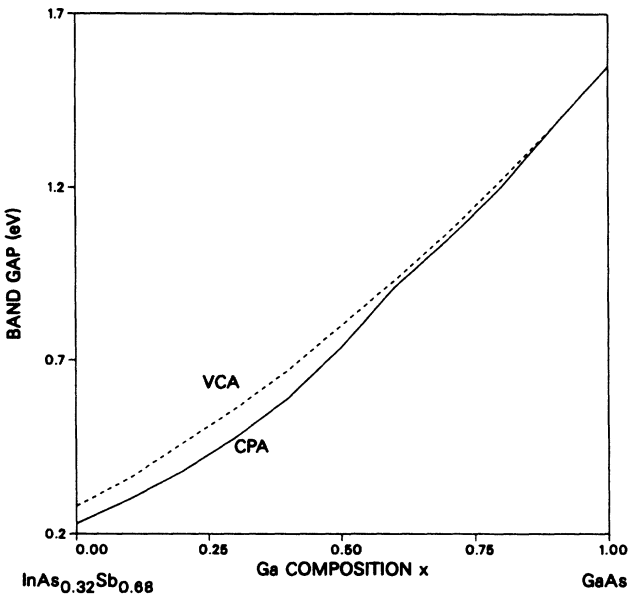

FIG. 7. CPA (solid curve) and VCA (dashed curve) energy-gap variation with Ga composition x for $In_{1-x}Ga_xAs_ySb_{1-y}$ lattice matched to GaAs ($x=1.471y-0.471$).

CPA bowing parameter is smaller by about 100 meV in our case for reasons just discussed. The large deviations between the band-gap bowing predicted in the VCA and the CPA show again that alloy disorder effects can be important for this alloy.

In Figs. 7 and 8, we also show, respectively, the band-gap and the bowing parameter variations with composition for InGaAsSb lattice matched to GaAs ($0\le x\le 1$, $0.32\le y\le 1$). In this case, the relation between x and y is $x=1.471y-0.471$. The size of the CPA bowing parameter here is similar to that for InGaAsP lattice matched to GaAs, and the shape of both the VCA and CPA bowing curves is approximately parabolic. The CPA band gap at an As composition of $y=0.32$ is 0.23 eV and when extrapolated to room temperature, this is in reasonable agreement with the data of Ref. 11. The deviation between the CPA and the VCA bowing parameters for this alloy are even larger than for InGaAsP lattice matched to

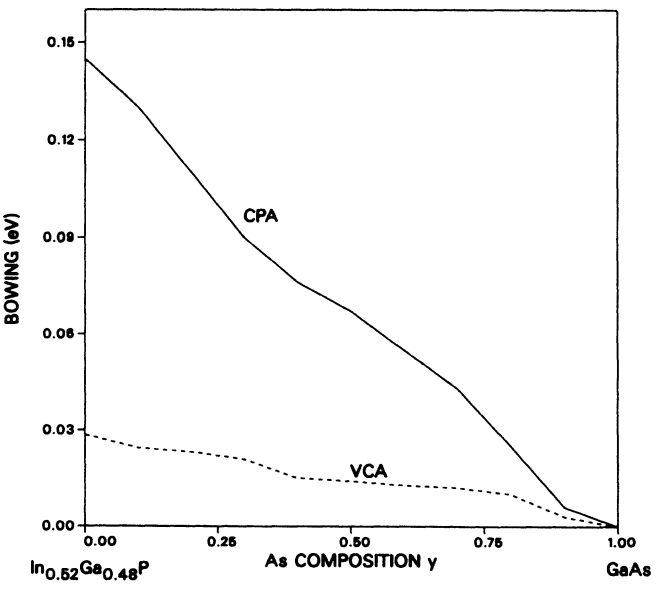

FIG. 6. CPA (solid curve) and VCA (dashed curve) band-gap bowing as a function of As composition y for $In_{1-x}Ga_xAs_yP_{1-y}$ lattice matched to GaAs ($0.42x-0.22y=0.20$).

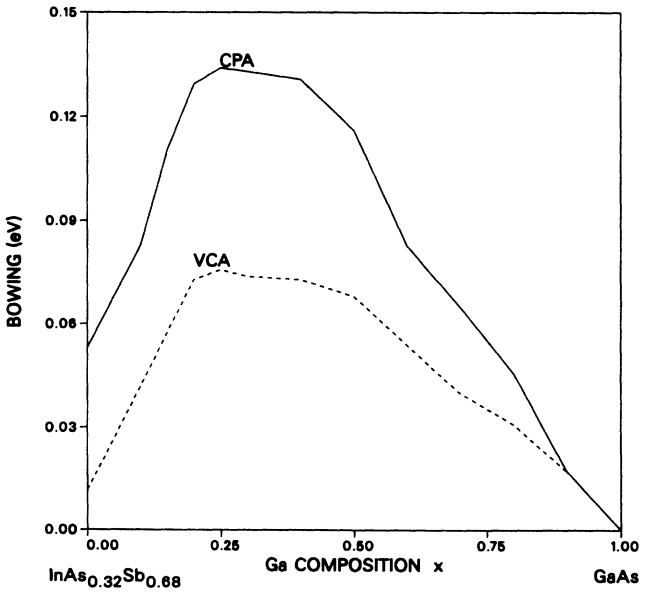

FIG. 8. CPA (solid curve) and VCA (dashed curve) band-gap bowing as a function of Ga composition x for $In_{1-x}Ga_xAs_ySb_{1-y}$ lattice matched to GaAs ($x=1.471y-0.471$).

TABLE II. Energy gaps (E_g) and band-gap-bowing parameters (b) calculated in both VCA and CPA for the four alloys $Al_xGa_{1-x}As_yP_{1-y}$, $Al_xGa_{1-x}As_ySb_{1-y}$, $In_{1-x}Ga_xAs_yP_{1-y}$, and $In_{1-x}Ga_xAs_ySb_{1-y}$ at various compositions x and y. All energies are in electron volts.

Alloy	x	0.25	0.25	0.25	0.50	0.50	0.50	0.75	0.75	0.75
	y	0.25	0.50	0.75	0.25	0.50	0.75	0.25	0.50	0.75
$Al_xGa_{1-x}As_yP_{1-y}$	b (VCA)	0.01	0.00	0.01	0.00	0.00	0.00	0.00	0.00	0.01
	b (CPA)	0.02	0.03	0.03	0.01	0.03	0.01	0.00	0.00	0.09
	E_g (VCA)	2.77	2.49	2.21	3.00	2.77	2.53	3.23	3.04	2.85
	E_g (CPA)	2.75	2.45	2.16	2.99	2.73	2.52	3.23	3.04	2.73
$Al_xGa_{1-x}As_ySb_{1-y}$	b (VCA)	0.01	0.01	0.01	0.00	0.01	0.01	0.01	0.01	0.01
	b (CPA)	0.01	0.04	0.19	0.00	0.01	0.07	0.02	0.01	0.01
	E_g (VCA)	1.26	1.47	1.69	1.56	1.80	2.04	1.86	2.13	2.39
	E_g (CPA)	1.26	1.44	1.44	1.56	1.79	1.95	1.84	2.12	2.39
$In_{1-x}Ga_xAs_yP_{1-y}$	b (VCA)	0.02	0.01	0.02	0.03	0.02	0.01	0.02	0.01	0.01
	b (CPA)	0.08	0.07	0.07	0.17	0.09	0.08	0.09	0.12	0.03
	E_g (VCA)	1.49	1.22	0.96	1.83	1.54	1.26	2.18	1.87	1.57
	E_g (CPA)	1.40	1.14	0.89	1.63	1.43	1.17	2.07	1.72	1.54
$In_{1-x}Ga_xAs_ySb_{1-y}$	b (VCA)	0.02	0.02	0.02	0.02	0.02	0.02	0.02	0.02	0.07
	b (CPA)	0.07	0.08	0.07	0.09	0.09	0.04	0.12	0.07	0.13
	E_g (VCA)	0.43	0.51	0.60	0.60	0.72	0.84	0.78	0.93	1.09
	E_g (CPA)	0.36	0.43	0.53	0.50	0.62	0.82	0.64	0.86	1.02

GaAs, again showing that alloy disorder is a stronger effect in the alloys containing Sb.

For the purpose of a general comparison, we display the VCA and CPA energy gaps and bowing parameters at similar compositions for the different alloys we have considered in Table II. The alloy AlGaAsP shows the least deviation between the VCA and CPA results, showing that disorder should be the least for this alloy. The maximum deviation in the energy gaps for this material is 0.06 eV at compositions of $x=0.25$ and $y=0.75$, and the corresponding maximum bowing parameter is 0.029 eV. These values are in good agreement with the size of the self-energies and disorder parameters for this alloy. The disorder in AlGaAsSb is larger than that in AlGaAsP, with a maximum deviation of the VCA and CPA energy band gaps of 0.16 eV at $x=0.25$ and $y=0.75$. The relative amounts of disorder in InGaAsP and InGaAsSb are about the same and are traceable to the difference in the s atomic energies between the cations In and Ga. These two quaternaries show more disorder than AlGaAsP and AlGaAsSb.

IV. CONCLUSION

We have presented a CPA formalism for the treatment of alloy disorder effects on the electronic properties of quaternary alloys with two disordered sublattices, and have presented the results of the application of this formalism to the four quaternary alloys AlGaAsP, AlGaAsSb, InGaAsP, and InGaAsSb. The CPA results are remarkably different from the VCA results, especially for InGaAsSb and InGaAsP. This is due to the relatively large alloy disorder in these alloys as characterized by their CPA self-energies. We have found that the band-gap bowing is greater in the InGaAsP lattice matched to GaAs than in the InP lattice-matched alloy in agreement with an earlier result.[6] In general, the values of the bowing parameters calculated here are small compared to previous calculations because the effects of interference between the scattering from one sublattice with the scattering from the other sublattice, which serve to reduce bowing, have been included in our results. Such effects, which should be present even for the perfectly random alloys we consider here, were neglected in previous calculations, where the scattering from the two sublattices was assumed to contribute additively to the bowing. Furthermore, we find that the CPA results are much closer to experimental data, especially for such quantities as the energy gap. This shows that the inclusion of alloy disorder effects is necessary in the study of the materials considered here.

From the discussion of the differences in s and p atomic energies, and also using the values of the bonding and antibonding energies from Table I for the antimonide and phosphide compounds, it is expected that alloys containing Sb and P will show larger disorder effects than the alloys studied here. We have shown this to be the case in calculations presented elsewhere.[26]

As discussed above, the inclusion of off-diagonal disorder effects, which were neglected here, would certainly be expected to change these results quantitatively. However, such effects are unlikely to change the trends we have predicted in the various properties as a function of the alloy compositions and from alloy to alloy. For example, such effects should not alter the result that alloy disorder effects are more important for the Sb containing alloys than for the others.

ACKNOWLEDGMENTS

We thank the Texas Tech University Graduate School for partial support of this work at its early stages.

APPENDIX

Equation (8) of the text is in general a matrix equation. However, the neglect of off-diagonal disorder means that the self-energy matrix Σ is diagonal with matrix elements σ_j. In the bonding-antibonding basis, we thus consider only two scalar self-energies σ_b and σ_a for the valence and conduction bands, respectively. Equation (8) then becomes a scalar equation which can be expanded to obtain

$$\begin{aligned}\sigma=&[x(1-y)(u_{AC}+u_{BC})(\varepsilon_{BD}-\varepsilon_{AD})-xy(u_{BD}+u_{AD})(\varepsilon_{AC}-\varepsilon_{BC})-y(u_{AD}+u_{AC})(\varepsilon_{BC}-\varepsilon_{BD})\\&-3\sigma^2+\sigma(u_{AC}+u_{BC}+u_{AD}+3u_{BD}+6\sigma)+\bar{\varepsilon}(\varepsilon_{AC}+\varepsilon_{BC}+\varepsilon_{AD}+3\varepsilon_{BD}-3\bar{\varepsilon})-\varepsilon_{BD}(\varepsilon_{AC}+\varepsilon_{BC}+\varepsilon_{AD})]g(E)\\&+g(E)[xyu_{AD}(\varepsilon_{AC}-\varepsilon_{BC})u_{BD}+x(y-1)u_{AC}(\varepsilon_{BD}-\varepsilon_{AD})u_{BC}+yu_{AC}(\varepsilon_{BC}-\varepsilon_{BD})u_{AD}\\&+u_{BD}(u_{BC}u_{AD}+u_{AC}u_{AD}+u_{AC}u_{BC})]g(E)-u_{AC}g(E)u_{BC}g(E)u_{AD}g(E)u_{BD}\ ,\end{aligned}$$

where the u_i's and the g_i's are as defined in the text. The above equation is a coupled, nonlinear, integral equation which is quartic in σ. Also, since this equation has the same form for both the conduction and valence bands for reasons already discussed in the text, we have dropped the subscript ($j=b,a$) for convenience and clarity.

*Present address: Department of Computer Science, University of Tennessee, Knoxville, TN 37996.

[1]C. E. Hurwitz and J. J. Hsieh, Appl. Phys. Lett. **32**, 487 (1978); J. J. Hsieh, *ibid.* **28**, 283 (1976).

[2]S. Yamakoshi, T. Sanada, O. Wada, I. Umebu, and T. Sakurai, Appl. Phys. Lett. **40**, 144 (1982).

[3]T. P. Pearsall, IEEE J. Quantum Electron **QE-16**, 709 (1980).

[4]M. Ichimura and A. Sasaki, Phys. Rev. B **36**, 9694 (1987).

[5]A. B. Chen and A. Sher, Phys. Rev. B **19**, 3057 (1979).

[6]V. B. Gera, R. Gupta, and K. P. Jain, Phys. Rev. B **36**, 9657 (1987).

[7]K. Nakajima, A. Yamaguchi, K. Akita, and T. Kotani, J. Appl. Phys. **49**, 5944 (1978).

[8]A. B. Chen and A. Sher, Phys. Rev. B **17**, 4726 (1978); **23**, 5360 (1981).

[9]Y.-T. Shen and C. W. Myles, J. Phys. Chem. Solids **48**, 1173 (1987).

[10]G. C. Osbourn, J. Vac. Sci. Technol. B **4**, 1423 (1986).

[11]C. G. Bethea, B. F. Levine, K. K. Choi, and A. Y. Cho, Appl. Phys. Lett. **51**, 1431 (1987).

[12]J. R. Gregg, C. W. Myles, and Y.-T. Shen, Phys. Rev. B **35**, 2532 (1987); J. R. Gregg, Ph.D. dissertation, Texas Tech University, 1988 (unpublished).

[13]S. M. Islam, Ph.D. dissertation, University of Notre Dame, 1987 (unpublished).

[14]G. B. Stringfellow and P. E. Greene, J. Phys. Chem. Solids **30**, 1779 (1969); E. A. Guggenheim, *Mixtures* (Oxford, London, 1952).

[15]A. Sher, M. van Schilgaarde, A.-B. Chen, and W. Chen, Phys. Rev. B **36**, 4279 (1987).

[16]P. Vogl, H. P. Hjalmarson, and J. D. Dow, J. Phys. Chem. Solids **44**, 365 (1983).

[17]R. J. Elliot, J. A. Krumhansl, and P. L. Leath, Rev. Mod. Phys. **46**, 465 (1974); H. Ehrenreich and L. M. Schwartz, in *Solid State Physics,* edited by H. Ehrenreich, F. Seitz, and D. Turnbull (Academic, New York, 1976), Vol. 31, p. 149.

[18]K. C. Hass, R. J. Lempert, and H. Ehrenreich, Phys. Rev. Lett. **52**, 77 (1984); R. J. Lempert, K. C. Hass, and H. Ehrenreich, Phys. Rev. B **36**, 1111 (1987).

[19]W. A. Harrison, *Electronic Structure and the Properties of Solids* (Freeman, San Francisco, 1980).

[20]N. J. Shevchek, J. Tejeda, and M. Cardona, Phys. Rev. B **9**, 2627 (1974).

[21]C. Alibert, G. Bordure, A. Laugier, and J. Chevallier, Phys. Rev. B **6**, 1301 (1972); S. S. Vishnubatla, B. Eyglunent, and J. C. Woolley, Can. J. Phys. **47**, 1661 (1969).

[22]R. E. Nahory, M. A. Pollack, and W. D. Johnston, Jr., Appl. Phys. Lett. **33**, 659 (1978).

[23]J. A. Van Vechten and T. K. Bergstresser, Phys. Rev. B **1**, 3351 (1970).

[24]R. Hill, J. Phys. C **7**, 521 (1974).

[25]T. P. Pearsall, in *GaInAsP Alloy Semiconductors,* edited by T. P. Pearsall (Wiley, New York, 1982), p. 295.

[26]S. N. Ekpenuma and C. W. Myles (unpublished).